Article

A Wireless Potentiostat Exploiting PWM-DAC for Interfacing of Wearable Electrochemical Biosensors in Non-Invasive Monitoring of Glucose Level

Antonio Vincenzo Radogna [1,*], Luca Francioso [2], Elisa Sciurti [2,*], Daniele Bellisario [2], Vanessa Esposito [2] and Giuseppe Grassi [3]

[1] Department of Experimental Medicine, University of Salento, Campus Ecotekne, Via per Monteroni s.n., 73100 Lecce, Italy
[2] Institute for Microelectronics and Microsystems, National Research Council of Italy (CNR-IMM), Campus Ecotekne, Via per Monteroni s.n., 73100 Lecce, Italy; lucanunzio.francioso@cnr.it (L.F.); daniele.bellisario@imm.cnr.it (D.B.); vanessa.esposito@imm.cnr.it (V.E.)
[3] Department of Innovation Engineering, University of Salento, Campus Ecotekne, Via per Monteroni s.n., 73100 Lecce, Italy; giuseppe.grassi@unisalento.it
* Correspondence: antonio.radogna@unisalento.it (A.V.R.); elisa.sciurti@imm.cnr.it (E.S.)

Abstract: In this paper, a wireless potentiostat code-named ElectroSense, for interfacing of wearable electrochemical biosensors, will be presented. The system is devoted to non-invasive monitoring of glucose in wearable medical applications. Differently from other potentiostats in literature, which use digital-to-analog converters (DACs) as discrete components or integrated in high-end microcontrollers, in this work the pulse width modulation (PWM) technique is exploited through PWM-DAC approach to generate signals. The ubiquitous presence of integrated PWM peripherals in low-end microcontrollers, which generally also integrate analog-to-digital converters (ADCs), enables both the generation and acquisition of read-out signals on a single cheap electronic device without additional hardware. By this way, system's production costs, power consumption, and system's size are greatly reduced with respect to other solutions. All these features allow the system's adoption in wearable healthcare Internet-of-things (IoT) ecosystems. A description of both the sensing technology and the circuit will be discussed in detail, emphasizing advantages and drawbacks of the PWM-DAC approach. Experimental measurements will prove the efficacy of the proposed electronic system for non-invasive monitoring of glucose in wearable medical applications.

Keywords: potentiostat; wearable; glucose; electrochemical; analog front-end circuit; PWM-DAC

1. Introduction

Recent advances in smaller, lower-powered technologies are fueling the revolution of portable electronic products [1]. Many Internet-of-Things (IoT) applications, in both consumer and healthcare markets, enable an unmatched interaction with smart environments, providing the users with massive amount of information, changing and adapting it according to their needs and preferences. IoT products are supported by development and pervasive deployment of smart electronic devices equipped with a microcontroller (MCU), a communication interface (wired or wireless), a power supply, and a set of sensors and actuators that are used to interface with the environment. A key innovation, leading to modern portable products, has been the introduction of wearable sensors and devices. Their adoption in low-cost point-of-care devices permits to avoid the use of bulky and expensive laboratory equipment for healthcare monitoring. A prominent benefit of this could be the decreasing of the number of hospital visits while increasing the quality of patient life [2]. Many sensing principles, such as enzyme field effect transistors (ENFETs) [3] and resonator-based biosensors [4], can be exploited to develop affordable and accurate

monitoring systems. However, their adoption in low-power wearable applications results unpractical since they require laboratory instrumentation which is not suitable for portable and low-power devices. In contrast, electrochemical biosensors are frequently adopted in wearable contexts as emerging technology for continuous and non-invasive monitoring of a wide range of analytes such as lactate, sodium, alcohol and glucose for diabetes monitoring [5,6]. An important application field is the therapeutic check through bodily fluids [6]. This correlates the pharmacokinetic properties of drugs with optimal outcomes by realizing customized dose regulations in real-time. Devices can track dynamic changes in pharmacokinetics behavior while assuring the medication of patients. Another field of application of wearable electrochemical biosensors is the abuse of drugs. Monitoring devices can serve as powerful screening tools in the hands of law enforcement agents to contrast drug trafficking and to support on-site forensic investigations. Regarding the glucose, the positive impact of real-time monitoring would concern the proper regulation of glucose homeostasis through correct insulin administration, eliminating the risk of patient's overdosing [7]. Research efforts over more than two decades were devoted for the development of non-invasive optical and electrochemical glucose monitoring [8]. However, despite of this, realizing a reliable and stable non-invasive sensing device for non-invasive glucose monitoring remains an elusive goal. The electronic systems for the interfacing and read-out of electrochemical sensors are called potentiostats. By considering a typical 3-electrodes electrochemical cell, a potentiostat operates by maintaining a potential on the working electrode (WE) with respect to the reference electrode (RE) and by measuring the current flowing between the WE and the counter electrode (CE).

Here, a low-cost wireless potentiostat, for interfacing of wearable electrochemical biosensors, is introduced. The device uses the PWM-DAC technique for the generation of excitation signal and it is adopted in the non-invasive monitoring of glucose level for wearable medical applications. The paper is organized as follows: Section 3 provides an overview the proposed system, emphasizing details on the circuit design, on the PWM-DAC technique, and on the sensing technology. The system is experimentally validated through the measurements reported in Section 4. Finally, Section 5 summarizes the findings.

2. Literature Review

Miniaturized potentiostats were adopted as monitoring devices for a multitude of analytes in the sweat [9]. For instance, in [10] a wireless and wearable potentiostat for cyclic voltammetry is described and tested with buffer solutions. The device shows a maximum read-out current of 500 μA and leverages on the Bluetooth wireless protocol for data communication. In addition to the Bluetooth MCU, the solution adopts a discrete digital-to-analog converter (DAC) for the signal generation. A similar solution is adopted in [11] where a portable potentiostat with USB communication is presented and tested with a dummy circuit. Another wireless potentiostat with discrete DAC is proposed in [12]. As an alternative approach, in [13] a monolithic solution is proposed by integrating the DAC in the same an ARM-Cortex-M4-based MCU. A different approach is used in the wearable solution presented in [5]. It leverages on the LMP91000, a well-known commercial integrated circuit acting as a programmable analog front-end (AFE) for electrochemical measurements. This component integrates all the useful circuits for the signal generation and acquisition from sensors. The mentioned works make use of high-end MCUs with integrated DAC or, alternatively, use a discrete DAC. These solutions account for high production costs of the system and for additional power consumption as well.

In this paper, a wireless potentiostat code-named ElectroSense, devoted to the interfacing of wearable electrochemical sensors for non-invasive detection of glucose, is described. As an extended version of [14], more details are provided on the system's design and implementation, both from the point of view of the circuit and the sensor. The device's key features lie in the technique for the generation of analog signals (current or voltage) responsible for the sensor's stimulation. A pulse-width-modulation-based digital-to-analog converter (PWM-DAC) technique is adopted instead of conventional voltage DAC. This

approach aims to use a single low-end MCU to implement both the signal generation and acquisition. This is possible since, differently from DACs, which are not integrated in cheap MCUs, the PWM peripheral is always available on chip. By this way, it is possible to save resources in terms of cost for the system's realization, power consumption of the device, and area occupation on printed circuit board (PCB).

3. System Overview

3.1. Sensing Technology

Modern electrochemical sensors exhibit relevant advantages such as low detection limit, in the picomoles range, fast response, and simple equipment for measurement. Thanks to their sensing principle, they can be miniaturized for full integration in wearable devices [15]. Here, electrochemical sensors are selected since they deliver accurate and real-time data regarding the chemical composition of its surroundings. The electrochemical glucose sweat sensor was fabricated by a standard fabrication process on a silicon wafer substrate with a circular chromium/gold 5 nm/200 nm film thickness) working electrode (8 mm diameter) and a titanium/platinum thin film (10 nm/300 nm thickness) pseudo-reference electrode deposited by e-beam evaporation. A photo of the realized sensor is depicted in Figure 1. The working electrode was functionalized with three different layers: a first electroactive layer of Prussian Blue (PB) was electrodeposited on the gold surface of the electrode; then a polymer solution of chitosan mixed with 20 mg/mL of the enzyme glucose oxidase (GOx) and gold nanourchins (GNU) was drop-coated on the PB film. Finally, the electrode was covered with a 5% Nafion solution to form a protective layer. The response of the sensor to glucose is mediated by GOx, incorporated into the chitosan membrane in the presence of gold nanourchins to enhance the sensor sensitivity. GOx catalyzes the production of hydrogen peroxide (H_2O_2) in proportion to glucose concentration according to the following equation:

$$\text{glucose} + \text{oxygen} \longrightarrow \text{gluconic acid} + \text{hydrogen peroxide} \tag{1}$$
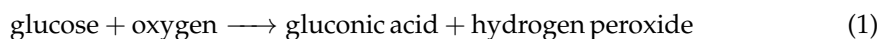
The amperometric detection of hydrogen peroxide usually take place at high potential (above 0.6 V vs. Ag/AgCl), but is interfered by many other substances present in the sample [16]. The PB layer acts as an "artificial peroxidase" allowing the reduction of H_2O_2 at low potential, avoiding the problem of interfering species. This produces an amperometric response which reflects the glucose concentration in the sample.
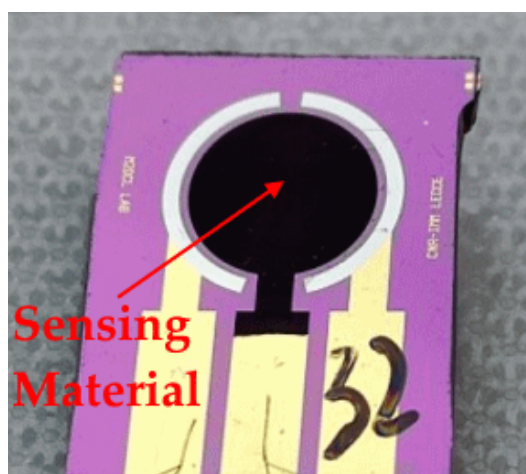

Figure 1. Fabricated electrochemical sensor.

3.2. Circuit Implementation

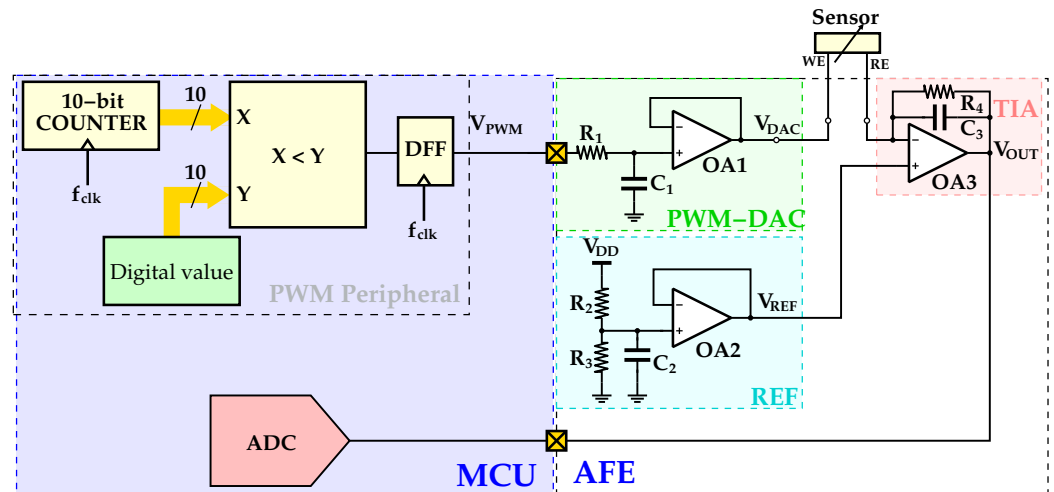Figure 2 shows a diagram of the ElectroSense circuit schematic.

Figure 2. Simplified circuit schematic of the designed ElectroSense wireless potentiostat.

The circuit is composed by the MCU section (left) and the AFE section (right). The first is responsible for the Bluetooth communication, the generation of the excitation signal, the analog-to-digital conversion, and for the control of system's operation. An ATmega328 microcontroller, manufactured by Atmel, was selected thanks to its wide availability on the market and for its low cost. It exhibits the following specifications: advanced RISC architecture, operating frequency of 16 MHz, 32 kB flash memory, 2 kB RAM memory, and a 1 kB EEPROM. Prominent features, useful to implement the desired functionality, are the 10-bit ADC and 6 PWM channels. Regarding the AFE section, it is responsible for the interfacing between the electrochemical sensor and the digital section. The excitation signal for the amperometry operation mode is generated through the PWM-DAC approach. This technique has been exploited in [17,18] in order to generate digitally controlled AC voltages with low requirements in terms of cost and hardware demand [19]. In brief, the PWM-DAC generates a desired analog voltage by filtering, with a low-pass filter, a PWM signal with a variable duty cycle (δ). In the recent years, this technique was exploited for high accuracy applications since modern chip manufacturers provide improved PWM modules with significantly high clock rates, thus enhancing the performance of the overall signal generation process [20]. The peripheral in the MCU, which is responsible for the pulse-width modulation, can be considered as an N_d-bit binary counter followed by an N_d-bit magnitude comparator [18]. A periodical digital ramp is available at the output of the counter with the following period:

$$T = \frac{2^{N_d}}{f_{clk}} \tag{2}$$

The desired output waveform from the PWM-DAC is obtained by comparing the output of the comparator (X input) with a digital word (Y input). As a result, the pulse width of the comparator output signal is proportional to the digital value. Finally, a D flip-flop is used to eliminate the transition glitches. The δ is defined as the ratio between the high-value interval and the overall period. Figure 3 depicts a generic PWM signal with increasing δ, where V_H and V_L are the high and low voltage values, respectively, of the signal, T_H is the high-value interval of the signal, and T is its period. Regarding the choice of the PWM frequency, it was selected equal to 7.8 kHz.
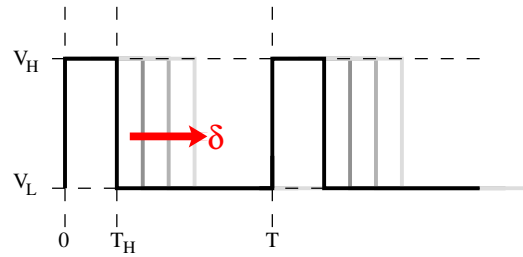
Figure 3. Generic PWM signal with increasing δ.

The PWM peripheral of the MCU provides a δ resolution of 10 bits. This means that the δ range from 0% to 100% is mapped in the integer range from 0 to 1023. The following expanded expression through Fourier analysis, for the V_{PWM} signal, is derived in [21]:

$$V_{PWM}(t) = [\delta \cdot V_{FS} - V_L] + \frac{2 \cdot V_{FS}}{\pi} \cdot sin(\delta \cdot \pi) \cdot cos\left(\frac{2\pi}{T} \cdot t - \delta \cdot \pi\right)$$
$$+ \sum_{n=2}^{\infty} \frac{2 \cdot V_{FS}}{n \cdot \pi} \cdot sin(\delta \cdot n \cdot \pi) \cdot cos\left(\frac{2\pi \cdot n}{T} \cdot t - \delta \cdot \pi \cdot n\right) \quad (3)$$

where V_{FS} is equal to $V_H - V_L$. The V_{PWM} waveform is then filtered in order to preserve the first term in (3). Since this term is proportional to the duty cycle, δ, by varying the latter from 0 to 100%, a desired output voltage, V_{DAC}, with voltage values from V_L to V_H is obtained. As depicted in the PWM-DAC subcircuit in Figure 2, the PWM signal is filtered by a low-pass filter to obtain the desired V_{DAC} voltage for the sensor excitation. This voltage is obtained through the following expression:

$$V_{DAC} = \frac{N_i}{2^{N_d} - 1} \cdot V_{FS} - V_{REF} \quad (4)$$

where N_i is the integer δ range from 0 to 1023, N_d is the PWM resolution equal to 10 bits, $V_{FS} = V_H - V_L$ is the full-scale voltage of the PWM-DAC set to 5 V, and V_{REF} is the reference voltage set to $V_{DD}/2$. The output signal can be a triangular waveform, useful as the potentiostat is in voltammetry mode, or a constant voltage, useful in amperometry mode. In order to keep a low number on components on PCB, a first-order passive RC filter was chosen and its sizing was performed according to [19]. The resistor and capacitor values have been selected equal to $10\,\mathrm{k\Omega}$ and $100\,\mathrm{nF}$, respectively. The filter's time constant, equal to 1 ms, was chosen much larger than the period of the PWM, which is about $130\,\mathrm{\mu s}$. This value is a trade-off between filtering efficacy, mandatory to obtain a small peak-to-peak ripple voltage, and settling time of the PWM-DAC. However, it can be specified that in the case of static excitation signal, the settling time does not really matter since the generated signal is constant. This is the case of the amperometry mode, whose measurements are described in Section 4.2. As already specified, the potentiostat was designed for the read-out of a 2-terminal electrochemical sensor. Specifically, while the output of the PWM-DAC is connected to the WE of the sensor, the RE is connected to the transimpedance amplifier for the current read-out. The latter block is identified as TIA in Figure 2. Basically, the TIA acts as a current-to-voltage converter in order to convert the output current from the sensor in a voltage for the ADC. From basic circuit theory, the output voltage of the TIA, V_{OUT}, can be expressed as:

$$V_{OUT} = V_{REF} - R_4 \cdot I_S(t) \quad (5)$$

where $I_S(t)$ is the output current from the sensor. The feedback resistor, R_4, is selected in order to prevent the opamp saturation and depends on the sensor's maximum output current according to (5). By considering a maximum output current from the sensor, I_{MAX}, equal to $10\,\mathrm{\mu A}$ and a rail-to-ral opamp with maximum V_{OUT} equal to 5 V, a R_4 resistor equal to $250\,\mathrm{k\Omega}$ was chosen. The C_4 capacitor, whose value is 1 nF, was added in feedback

to the OA3 opamp in order to ensure its stability. The following expression is used to convert the output word from the ADC, N_o, to the sensor's output current, I_S:

$$I_S = \frac{V_{REF} - \dfrac{N_o \cdot V_{FS}}{2^{N_a} - 1}}{R_4} \tag{6}$$

where N_a is the resolution of the used ADC, equal to 10 bits. Regarding the V_{REF} voltage generation, it has been obtained through a buffered voltage divider with the R_2 and R_3 resistor being both equal to $100\,\text{k}\Omega$. The N_o digital words are processed through a basic moving average filter which was implemented on the MCU. This filter works as low-pass filter and it represents an efficient way to filter the sensor's signal from electronic noise, environmental interferences, non-idealities of electronic components, etc. This is also useful in order to attenuate the ripple contribution. Regarding the operational amplifier (opamp) selection, an OPA2344 has been selected since it satisfies the requirements in terms of gain, bandwidth and input/output rail-to-rail operation. The latter feature is useful in order to use the entire full-scale of the ADC.

The wireless communication is ensured through an HC-05 Bluetooth module. This is a widely adopted device for the easy wireless replacement of serial RS232 communications. It uses the $2.4\,\text{GHz}$ frequency band with a data rate up to 1 Mbps and it can operate in a range of $10\,\text{m}$.

A photo of the realized system is depicted in Figure 4. The figure shows the UART connector for the HC-05 module and the screw terminal for the 2-electrodes electrochemical sensor. The realized module also features a power section for driving valves and pumps for other intended uses outside wearable systems [22].
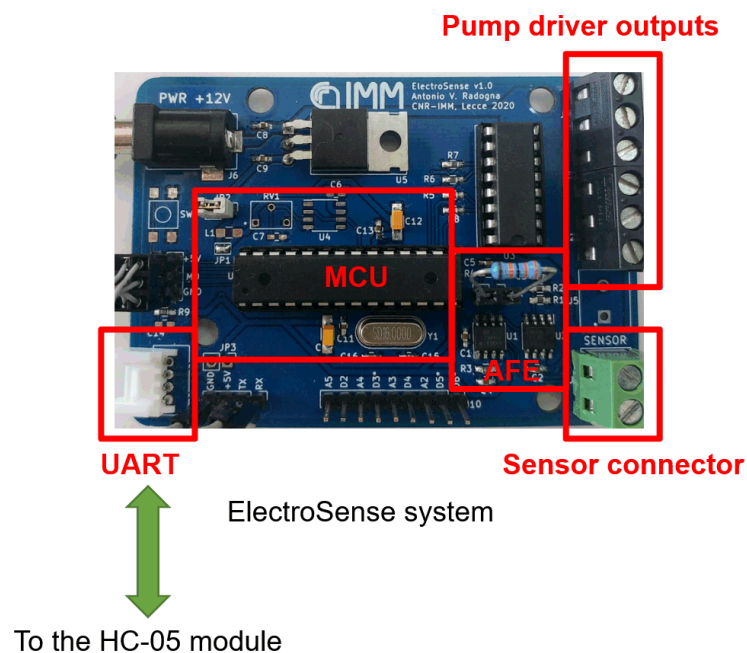

Figure 4. Photo of the ElectroSense mainboard.

The portable operation of the wearable system is possible thanks to a battery.

4. Experimental Measurements

4.1. Potentiostat Electrical Test

A first electrical test was conducted on the wireless potentiostat in order to verify the correct signal generation and acquisition. A self-check for cyclic voltammetry mode was conducted by generating 3 periods of a triangular waveform with a $100\,\text{mV}\,\text{s}^{-1}$ slope and a

voltage range from $-1\,\text{V}$ to $1\,\text{V}$. The WE and RE electrodes were connected together with OA3 opamp connected as voltage follower.

The result of this self-check is then captured by a serial terminal software by means of Bluetooth communication. Figure 5 shows the desired triangular waveform for the cyclic voltammetry. The signal range goes from $1.5\,\text{V}$ to $3.5\,\text{V}$ and it corresponds to the $+1\,\text{V} \div -1\,\text{V}$ by considering the V_{REF} (i.e., $2.5\,\text{V}$) as zero. A gaussian random process, with measured standard deviation equal to about $40\,\text{mV}$, can be used to describe the voltage ripple in the PWM-DAC signal. This voltage ripple is the main drawback of the PWM-DAC approach, resulting from the filtering of the PWM signal. A mean current consumption of $30\,\text{mA}$ was measured during the read-out operation, corresponding to a power consumption of $150\,\text{mW}$ at $5\,\text{V}$ supply voltage. The reduced power consumption makes the system suitable for adoption in healthcare Internet-of-Things (IoT) ecosystems.
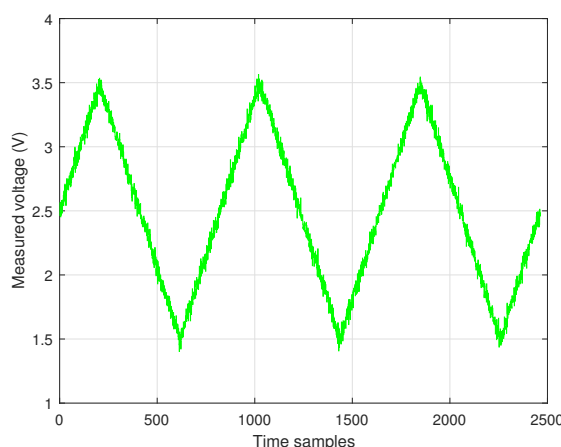

Figure 5. Self-check for signal generation and acquisition.

4.2. Amperometric Measurements with Electrochemical Sensor

The preliminary electrochemical measurements were performed using a commercial potentiostat/galvanostat (Ivium Vertex One, Ivium Technologies B.V., Eindhoven, The Netherlands). For electrochemical characterization of PB layer, cyclic voltammetry measurement were performed from $0.35\,\text{V}$ to $-0.05\,\text{V}$ vs. Ag/AgCl in a solution containing $100\,\text{mM}$ KCl and $100\,\text{mM}$ HCl, and the typical oxidation/reduction peaks of PB are shown in Figure 6a. For the detection of glucose, chronoamperometric measurements were performed at $-0.4\,\text{V}$ vs. Pt with the two-electrode integrated sensor.

The measurement through the commercial instrument and with different glucose concentrations (0.3–9.37 mM in PBS, pH 7.4) are reported in Figure 6b. The enzymatic sensor exhibited a sensitive response to the addition of the analyte with a linear decrease in current as glucose concentrations increased. The linear relationship between the absolute current and the different glucose concentrations is described by the fitting equation $y = (0.68 \pm 0.02) \cdot x + (1.74 \pm 0.05)$ with a correlation coefficient of 0.99 (Figure 6c). The selectivity of the developed glucose electrochemical sensor was evaluated by performing chronoamperometric measurements in the presence of typical interfering species in sweat including NaCl ($0.1\,\text{mM}$), KCl ($0.1\,\text{mM}$), uric acid ($1\,\text{mM}$) and lactic acid ($3\,\text{mM}$). Figure 6d shows the excellent selectivity of the sensor, with a non-significant increase in the response (%) in the presence of lactic acid.

The sensor was also measured through ElectroSense potentiostat and the results are depicted in Figure 7. From the figure, it can be noted a very good accordance in the measurements between the commercial instrument and the ElectroSense potentiostat.
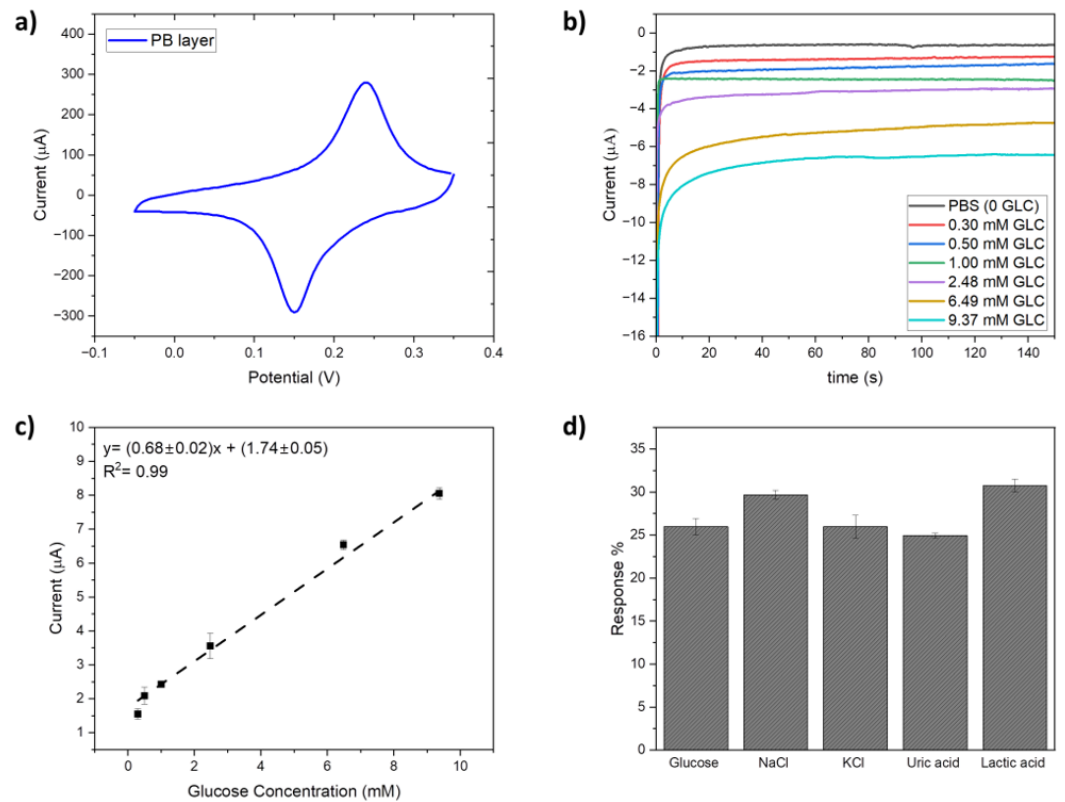
Figure 6. Electrochemical measurements: (**a**) cyclic voltammetry of the PB layer in KCl/HCl (0.1 M); (**b**) chronoamperometric response of the glucose sensor with different glucose (GLC) concentrations (0.3–9.37 mM through the commercial instrument); (**c**) calibration curve of the glucose sensor at increasing concentrations of glucose; (**d**) variation in amperometric response (%) for glucose (0.5 mM) and added interfering species (0.1 mM NaCl, 0.1 mM KCl, 1 mM uric acid, 3 mM lactic acid).
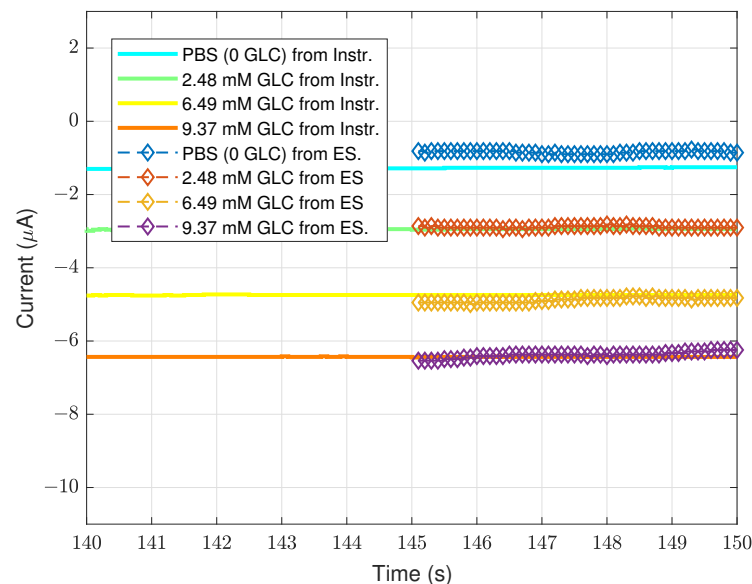
Figure 7. Real-time sensor measurements with different glucose (GLC) concentrations through the ElectroSense (ES) potentiostat. The measurement are compared with those from the commercial instrument.

4.3. Measurements in Real Conditions

The realized electrochemical sensor was integrated in a commercial patch used in medical practice, as depicted in Figure 8. Real wearable conditions were reproduced in

laboratory environment by testing the system, composed by electrochemical sensor and ElectroSense wireless potentiostat, in artificial sweat. First, agarose-based hydrogels were developed as sweat collectors on which the glucose sensors performed the electrochemical measurements. An agarose hydrogel at a concentration of 2% was prepared by dissolving the agarose powder (Sigma-Aldrich, St. Louis, MO, USA) in water, boiled and poured in a petri dish. After gelling for 2 h at room temperature, the hydrogel was cut into 1 cm^2 sheets, about 1 mm thick. The remarkable hydrophilicity of the agarose hydrogel facilitates the absorption of aqueous solutions, allowing it to be used as a sweat reservoir. The captured sweat solution is then released onto the nanocomposite polymeric layer of the electrochemical sensor which is able to quantify the glucose. An artificial sweat solution was prepared as reported in [23] by dissolving NaCl (0.5 wt%), urea (0.1 wt%), lactic acid (0.1 wt%) and glucose at a concentration of 0.25 mM in distilled water. The agarose hydrogel sheets were immersed in the artificial sweat containing glucose for 1 h and then used for the sensing measurements, after a removal of excess solution by a gentle contact with filter paper to avoid measurements artifacts. A number of hydrogels were soaked in a sweat solution without glucose as negative control. Amperometric measurements were performed with both the commercial potentiostat and the ElectroSense potentiostat by applying the sweat-impregnated hydrogel to the sensor surface. Figure 9 shows the electrochemical response of the sensor from the artificial sweat impregnated hydrogel (blue plots) and the sweat containing glucose (red plots). The results also confirmed the response of the glucose sensor in sweat, showing an increased current change in the presence of glucose and the accordance between the measurements with the ElectroSense potentiostat and the commercial instrument. The obtained results demonstrate the ability of the electrochemical sensor to quantify glucose in artificial sweat and the possibility of combining it with the wireless potentiostat to set up a potential system for wearable glucose monitoring.
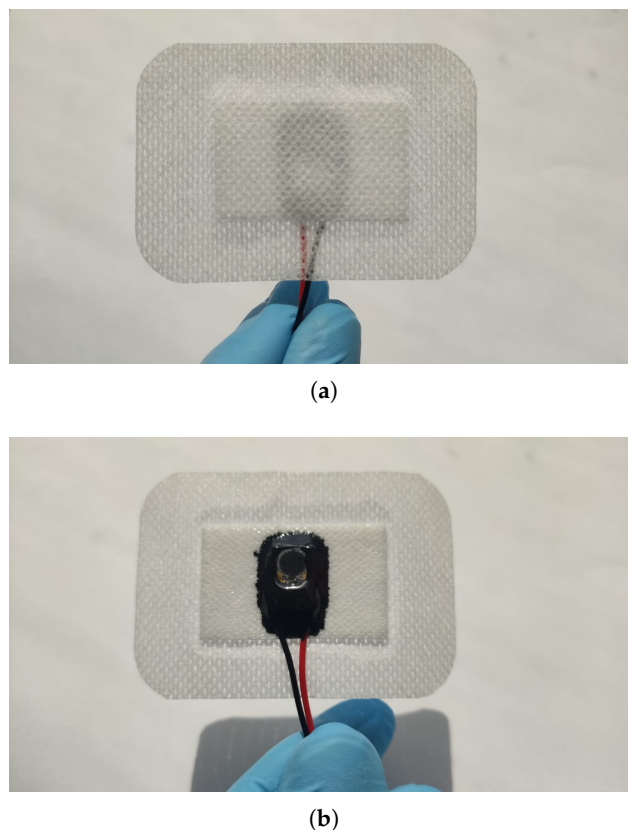

(**a**)

(**b**)

Figure 8. Realized adhesive patch with integrated sensor. (**a**) External side. (**b**) Internal side.
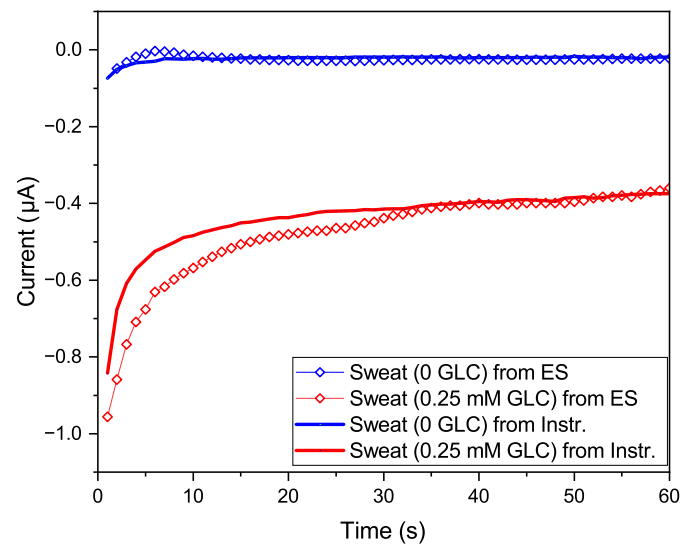
Figure 9. Amperometric responses of the electrochemical sensor to glucose (0.25 mM) in artificial sweat. The measurements were taken with both the ElectroSense potentiostat and the commercial instrument.

Table 1 shows a comparison between the proposed potentiostat and other works in literature.

Table 1. Comparison with the state-of-the-art.

	Meas. Approach	Terminals No.	Application	Signal Generation	Communication
[5]	Cyclic voltammetry, square wave voltammetry, chronoamperometry, and normal pulse voltammetry	3	Anti-cocaine aptamer	External AFE and DAC	USB (Wired)
[10]	Cyclic voltammetry and chronoamperometry	3	Healthcare	External 16-bit DAC	BLE
[11]	Cyclic voltammetry	3	Generic electroch. measurements	External 16-bit DAC	USB (Wired)
[12]	Cyclic voltammetry, chronoamperometry, and square wave voltammetry	3	Generic electroch. measurements	Integrated DAC into the MCU	BLE
[13]	Cyclic voltammetry, linear sweep voltammetry, chronoamperometry, chronocoulometry	2	Macroelectrode and ultramicroelectrode studies	Integrated DAC into the MCU	USB (Wired)
This work	**CV and chronoamperometry**	**2**	**Wearable Healthc.**	**PWM-DAC**	**Bluetooth V2.0**

5. Conclusions

In this paper, a low-cost wireless potentiostat, for interfacing of wearable electrochemical biosensors, was proposed. The device, code-named ElectroSense, is adopted in the non-invasive monitoring of glucose level and it is aimed to wearable medical applications. Differently from other wireless potentiostats in literature, which use high-end microcontrollers with integrated DACs, the ElectroSense potentiostat uses the PWM-DAC approach for signal generation. This design choice permits to save production costs since a low-end microcontroller with a PWM peripheral can be adopted for both the signal generation and acquisition. Moreover, power consumption of the circuit and area occupation on PCB are greatly reduced as well. All these features make the system suitable for the adoption in healthcare IoT ecosystems. The wireless potentiostat was coupled with a wearable electrochemical biosensor and the resulting amperometric measurements show a good accordance with those obtained by commercial laboratory equipment. Finally, measurements in artificial sweat were reported, proving the efficacy of the proposed device for

non-invasive measurements of glucose in wearable medical applications. A future upgrade of the work will include a constant current generation circuit, on the ElectroSense board, for iontophoretic sweating stimulation.

Institutional Review Board Statement: Not applicable.

Informed Consent Statement: Not applicable.

Data Availability Statement: No new data were created or analyzed in this study. Data sharing is not applicable to this article.

Conflicts of Interest: The authors declare no conflicts of interest.

Abbreviations

The following abbreviations are used in this manuscript:

ADC	analog-to-digital converter
AFE	analog front end
CE	counter electrode
DAC	digital-to-analog converter
GNU	gold nanourchins
GOx	glucose oxidase
IoT	Internet-of-things
MCU	microcontroller unit
PWM-DAC	pulse-width-modulation-based digital-to-analog converter
RE	reference electrode
PCB	printed circuit board
TIA	transimpedance amplifier
WE	working electrode

References

1. Shumba, A.T.; Montanaro, T.; Sergi, I.; Fachechi, L.; Vittorio, M.D.; Patrono, L. Leveraging IoT-Aware Technologies and AI Techniques for Real-Time Critical Healthcare Applications. *Sensors* **2022**, *22*, 7675. [CrossRef] [PubMed]
2. Xu, W.; Althumayri, M.; Mohammad, A.; Ceylan Koydemir, H. Foldable low-cost point-of-care device for testing blood coagulation using smartphones. *Biosens. Bioelectron.* **2023**, *242*, 115755. [CrossRef] [PubMed]
3. Ravariu, C.; Parvulescu, C.C.; Manea, E.; Tucureanu, V. Optimized Technologies for Cointegration of MOS Transistor and Glucose Oxidase Enzyme on a Si-Wafer. *Biosensors* **2021**, *11*, 497. [CrossRef] [PubMed]
4. Yue, W.; Kim, E.S.; Zhu, B.H.; Chen, J.; Liang, J.G.; Kim, N.Y. Permittivity-Inspired Microwave Resonator-Based Biosensor Based on Integrated Passive Device Technology for Glucose Identification. *Biosensors* **2021**, *11*, 508. [CrossRef] [PubMed]
5. Hoilett, O.S.; Walker, J.F.; Balash, B.M.; Jaras, N.J.; Boppana, S.; Linnes, J.C. KickStat: A Coin-Sized Potentiostat for High-Resolution Electrochemical Analysis. *Sensors* **2020**, *20*, 2407. [CrossRef] [PubMed]
6. Teymourian, H.; Parrilla, M.; Sempionatto, J.R.; Montiel, N.F.; Barfidokht, A.; Echelpoel, R.V.; Wael, K.D.; Wang, J. Wearable Electrochemical Sensors for the Monitoring and Screening of Drugs. *ACS Sens.* **2020**, *5*, 2679–2700. [CrossRef] [PubMed]

7. Lee, H.; Song, C.; Hong, Y.S.; Kim, M.S.; Cho, H.R.; Kang, T.; Shin, K.; Choi, S.H.; Hyeon, T.; Kim, D.H. Wearable/disposable sweat-based glucose monitoring device with multistage transdermal drug delivery module. *Sci. Adv.* **2017**, *3*, e1601314. [CrossRef] [PubMed]

8. Kim, J.; Campbell, A.S.; Wang, J. Wearable non-invasive epidermal glucose sensors: A review. *Talanta* **2018**, *177*, 163–170. [CrossRef] [PubMed]

9. Gao, W.; Emaminejad, S.; Nyein, H.Y.Y.; Challa, S.; Chen, K.; Peck, A.; Fahad, H.M.; Ota, H.; Shiraki, H.; Kiriya, D.; et al. Fully integrated wearable sensor arrays for multiplexed in situ perspiration analysis. *Nature* **2016**, *529*, 509–514. [CrossRef] [PubMed]

10. Ahmad, R.; Wolfbeis, O.S.; Alshareef, H.N.; Salama, K.N.; Surya, S.G.; Sales, J.B.; Mkaouar, H.; Catunda, S.Y.C.; Belfort, D.R.; Lei, Y.; et al. KAUSTat: A Wireless, Wearable, Open-Source Potentiostat for Electrochemical Measurements. In Proceedings of the 2019 IEEE SENSORS, Montreal, QC, Canada, 27–30 October 2019; IEEE: New York, NY, USA, 2019. [CrossRef]

11. Setiyono, R.; Lestari, T.F.H.; Anggraeni, A.; Hartati, Y.W.; Bahti, H.H. UnpadStat Design: Portable Potentiostat for Electrochemical Sensing Measurements Using Screen Printed Carbon Electrode. *Micromachines* **2023**, *14*, 268. [CrossRef] [PubMed]

12. Ainla, A.; Mousavi, M.P.S.; Tsaloglou, M.N.; Redston, J.; Bell, J.G.; Fernández-Abedul, M.T.; Whitesides, G.M. Open-Source Potentiostat for Wireless Electrochemical Detection with Smartphones. *Anal. Chem.* **2018**, *90*, 6240–6246. [CrossRef] [PubMed]

13. Glasscott, M.W.; Verber, M.D.; Hall, J.R.; Pendergast, A.D.; McKinney, C.J.; Dick, J.E. SweepStat: A Build-It-Yourself, Two-Electrode Potentiostat for Macroelectrode and Ultramicroelectrode Studies. *J. Chem. Educ.* **2019**, *97*, 265–270. [CrossRef]

14. Radogna, A.V.; Francioso, L.; Sciurti, E.; Bellisario, D.; Esposito, V.; Grassi, G. ElectroSense: A Low-cost Wearable Potentiostat for Real-time Monitoring of Glucose Level. In Proceedings of the 2023 8th International Conference on Smart and Sustainable Technologies (SpliTech), Split, Croatia, 20–23 June 2023; pp. 1–5. [CrossRef]

15. Baranwal, J.; Barse, B.; Gatto, G.; Broncova, G.; Kumar, A. Electrochemical Sensors and Their Applications: A Review. *Chemosensors* **2022**, *10*, 363. [CrossRef]

16. Vidal, J.C.; Espuelas, J.; Garcia-Ruiz, E.; Castillo, J.R. Amperometric cholesterol biosensors based on the electropolymerization of pyrrole and the electrocatalytic effect of Prussian-Blue layers helped with self-assembled monolayers. *Talanta* **2004**, *64*, 655–664. [CrossRef] [PubMed]

17. Wright, P.; Pickering, J. An AC voltage standard based on a PWM DAC. *IEEE Trans. Instrum. Meas.* **1999**, *48*, 457–461. [CrossRef]

18. Halper, C.; Heiss, M.; Brasseur, G. Digital-to-analog conversion by pulse-count modulation methods. *IEEE Trans. Instrum. Meas.* **1996**, *45*, 805–814. [CrossRef]

19. Pejovic, P. Output Voltage Filtering in Pulse Width Modulation Based D/A Converters. In Proceedings of the 2018 International Symposium on Industrial Electronics (INDEL), Banja Luka, Bosnia and Herzegovina, 1–3 November 2018; IEEE: New York, NY, USA, 2018. [CrossRef]

20. Thilakarathne, C.; Meegahapola, L.; Fernando, N.; Niakinezhad, M. PWM DAC based Input System for Synchrophasor Algorithm Testing. In Proceedings of the 2018 8th International Conference on Power and Energy Systems (ICPES), Colombo, Sri Lanka, 21–22 December 2018; pp. 93–97. [CrossRef]

21. Wang, Y.; Cheng, F.; Zhou, Y.; Xu, J. Analysis of double-T filter used for PWM circuit to D/A converter. In Proceedings of the 2012 24th Chinese Control and Decision Conference (CCDC), Taiyuan, China, 23–25 May 2012; pp. 2752–2756. [CrossRef]

22. Radogna, A.V.; Latino, M.E.; Menegoli, M.; Prontera, C.T.; Morgante, G.; Mongelli, D.; Giampetruzzi, L.; Corallo, A.; Bondavalli, A.; Francioso, L. A Monitoring Framework with Integrated Sensing Technologies for Enhanced Food Safety and Traceability. *Sensors* **2022**, *22*, 6509. [CrossRef] [PubMed]

23. Eldamak, A.R.; Thorson, S.; Fear, E.C. Study of the Dielectric Properties of Artificial Sweat Mixtures at Microwave Frequencies. *Biosensors* **2020**, *10*, 62. [CrossRef] [PubMed]